ISSN 2723-6471

Optimized Deep Learning method for Enhanced Medical Diagnostics of Polycystic Ovary Syndrome Detection

M. Praneesh[1,*], N. Nivetha[2], Siti Sarah Maidin[3], Wu Ge[4]

[1]*Sri Ramakrishna College of Arts and Science, Nava India, Coimbatore and 641006, India*

[2]*Vidyasagar College of Arts and Science, Udumelpet and 642126, India*

[3]*Faculty of Data Science and Information Technology (FDSIT), INTI International University, Nilai, Malaysia*

[4]*Faculty of Liberal Arts, Shinawatra University, Thailand*

(Received: June 23, 2024; Revised: July 19, 2024; Accepted: August 24, 2024; Available online: September 17, 2024)

Abstract

This paper explores Polycystic Ovary Syndrome (PCOS), a common hormonal disorder caused by elevated androgen levels, which affects women's reproductive health. The primary objective is to enhance early detection and diagnosis of PCOS using advanced machine learning techniques. To achieve this, the study utilizes VGG19 Net, integrated with various machine learning algorithms, to classify ultrasound images of the ovaries. The research involves analyzing ultrasound scans to differentiate between benign and potentially cancerous cysts. The contribution of this study lies in its novel application of VGG19 Net, which achieved an accuracy rate of 96% compared to other techniques: Random Forest (94%), Logistic Regression (91%), Bayesian Classifier (81%), Support Vector Machine (92%), and Artificial Neural Network (90%). The findings indicate that VGG19 Net outperforms traditional methods in precision and accuracy, with a significant improvement in detecting early-stage PCOS. This approach not only provides a clearer diagnostic image but also enables timely intervention, thus addressing the challenge of distinguishing between benign and malignant cysts more effectively. The results underscore the potential of VGG19 Net in revolutionizing PCOS diagnosis through enhanced image classification, offering a valuable tool for medical practitioners.

Keywords: PCOS, Convolutional Neural Networks, Hormone Imbalance, Feature Extraction, Process Innovation, Inclusive Health

1. Introduction

In contemporary society, disorders affecting the female reproductive system have garnered increasing attention due to their profound impact on women's health and well-being [1]. These disorders encompass a spectrum of conditions affecting various reproductive organs, including the uterus, vagina, cervix, and ovaries. Among these, Polycystic Ovary Syndrome (PCOS) emerges as a prevalent and complex endocrine disorder, affecting a significant portion of the female population worldwide [2]. PCOS is particularly noteworthy for its disruptive effects on hormonal balance, menstrual regularity, and fertility, thereby posing substantial challenges to affected individuals and healthcare providers alike [3]. The onset of PCOS typically occurs during adolescence or early adulthood, with symptoms often manifesting during the reproductive years [4]. Characterized by hormonal imbalances, irregular menstrual cycles, and the formation of cysts on the ovaries, PCOS presents a multifaceted clinical picture that necessitates careful evaluation and management [5]. Hormonal fluctuations, particularly elevated levels of androgens such as testosterone, contribute to the distinctive features of PCOS, including acne, hirsutism, and infertility [6]. These manifestations not only impact reproductive health but also exert systemic effects, such as insulin resistance and metabolic disturbances, further complicating the clinical course of the syndrome [7].

Despite its prevalence and clinical significance, diagnosing PCOS remains a challenge due to the heterogeneity of its presentation and the absence of a definitive diagnostic test [8]. Diagnosis typically relies on a combination of clinical evaluation, laboratory investigations, and imaging studies, with emphasis placed on identifying characteristic

***Corresponding author: M.Praneesh (raja.praneesh@gmail.com)**
DOI: https://doi.org/10.47738/jads.v5i3.368

symptoms and biochemical abnormalities [9]. Sonographic imaging plays a crucial role in visualizing ovarian morphology and detecting the presence of cysts, aiding in the diagnostic process [10]. Early detection and intervention are paramount in managing PCOS and mitigating its associated complications. Timely identification of the syndrome allows for the implementation of tailored treatment strategies aimed at restoring hormonal balance, improving menstrual regularity, and addressing fertility concerns [11]. Moreover, addressing modifiable risk factors, such as obesity and insulin resistance, can help alleviate symptoms and reduce the long-term health risks associated with PCOS [12].

Furthermore, the impact of PCOS extends beyond its physiological manifestations, encompassing significant psychosocial and quality-of-life implications for affected individuals [13]. Women with PCOS often experience heightened levels of anxiety, depression, and body image concerns, stemming from both the visible symptoms of the disorder and the challenges associated with fertility and reproductive health [14]. These psychosocial factors not only exacerbate the burden of illness but also underscore the importance of holistic, patient-centered approaches to PCOS care. Addressing the emotional and psychological well-being of individuals with PCOS is therefore integral to comprehensive management strategies, emphasizing the need for multidisciplinary collaboration and tailored support services [15].

Moreover, the epidemiological landscape of PCOS underscores the urgent need for improved diagnostic methodologies and therapeutic interventions to address the growing burden of this disorder. With an estimated prevalence ranging from 5% to 20% globally, PCOS represents one of the most common endocrine disorders affecting women of reproductive age [16]. Furthermore, emerging evidence suggests that PCOS is associated with an increased risk of various long-term health complications, including cardiovascular disease, type 2 diabetes, and endometrial cancer, highlighting the far-reaching consequences of this syndrome [17]. As such, efforts to enhance PCOS detection, optimize treatment strategies, and mitigate associated health risks are of paramount importance in promoting women's health and well-being across the lifespan [18].

In recent years, the advent of advanced computational techniques, particularly deep learning algorithms, has provided new avenues for enhancing the detection and classification of PCOS [19]. Leveraging large datasets encompassing clinical, imaging, and biochemical parameters, these algorithms offer the potential to improve diagnostic accuracy and facilitate personalized management approaches. By harnessing the power of artificial intelligence, researchers can explore novel biomarkers, refine diagnostic criteria, and develop predictive models to guide clinical decision-making in PCOS [20].

Against this backdrop, this paper presents a comparative analysis of deep learning algorithms for PCOS detection, focusing on their performance in classifying and predicting the syndrome based on diverse data sources. Through an in-depth examination of machine learning techniques, including CNNs, logistic regression, random forest, Bayesian classifiers, SVMs, and ANNs, this study aims to evaluate their efficacy in identifying key features associated with PCOS. Additionally, the integration of deep learning models with established imaging modalities, such as VGG 19 Net, offers a promising avenue for enhancing diagnostic accuracy and refining our understanding of PCOS path physiology.

In summary, this research endeavors to elucidate the role of deep learning algorithms in advancing PCOS diagnosis and management, highlighting their potential to transform clinical practice and improve patient outcomes. By harnessing the synergistic capabilities of artificial intelligence and medical imaging, we aim to foster innovation in the field of reproductive endocrinology and empower healthcare providers with tools for more precise and personalized care delivery.

2. Related Work

In the reproductive system of women, infertility is a significant issue that can result from the inhibition of follicle maturation, affecting follicle counts in the ovary [1]. For diagnosing PCOS, the number and size of follicles are crucial. Accurate detection of PCOS is essential and can be time-consuming. Typically, stereology calculations, classification, and feature extraction methods are employed for detection. One competitive model proposed by Zhang et al. [8] detects Polycystic Ovary from ultrasound images using a Gabor wavelet model and a competitive neural network for feature

extraction. This network combines Max net with Hemming net, optimizing data classification with ultrasound features to improve time efficiency and accuracy.

PCOS, a prominent disorder leading to infertility globally, can be prevented if detected at an early stage. Diagnostic imaging of the ovary is required for follicle analysis, but manual detection methods are error-prone, time-consuming, and laborious [9]. To address these issues, a hybrid model using Particle Swarm Optimization (PSO) with ANN for automatic follicle classification was introduced by Yılmaz and Özmen [11]. This approach utilizes the Lee filter for de-speckling ultrasound images, extracts features, and applies PSO to select significant features, which are then used to train a multilayer Perceptron ANN, achieving improved sensitivity, specificity, and accuracy.

In recent advancements, image recognition methodologies have been employed for disease diagnosis in medical fields. A probabilistic approach introduced by Jarrett et al. [10] enhances PCOS detection by employing kernel-based learners. This method segments images into grids, evaluates texture features and grayscale for each grid, and represents each image as a score matrix. The feature vectors derived from this matrix are then analyzed using a probabilistic model and transformed into SVM kernel features for PCOS detection, improving diagnostic outcomes.

The research conducted by Nazarudin et al. [1] addresses the significance of automated follicle identification in diagnosing PCOS. Their paper highlights the critical need for accurate follicle detection to facilitate appropriate medical interventions. Ultrasound imaging emerges as a pivotal diagnostic modality due to its non-invasive nature and cost-effectiveness. However, manual identification of follicles is impeded by speckle noise, resulting in time-consuming and error-prone analyses. The review examines various methodologies proposed by researchers to automate follicle identification, aiming to streamline the diagnostic process for medical practitioners. Despite advancements in this field, certain challenges persist, including the oversight of small or adjacent follicles, which could significantly impact treatment strategies. Furthermore, discrepancies in pre-processing filtering algorithms contribute to variations in evaluation parameters across studies. The review underscores the necessity for continued research efforts to develop robust speckle noise removal techniques and explore innovative approaches for identifying smaller and adjacent follicles in ovarian ultrasound images. Such endeavors are crucial for enhancing the accuracy and efficacy of PCOS diagnosis and treatment protocols [1].

Yılmaz and Özmen [11] investigated follicle detection for PCOS using image processing methods. They compared two approaches: one with noise filtering, contrast adjustment, binarization, and morphological processes, and another using Gaussian Filter and Wavelet Transform for noise reduction. Their evaluation revealed that the Wiener Filter and Gaussian Filter yielded the most accurate results. They suggest adaptive thresholding for improved contrast settings and future research to enhance PCOS classification by extracting features from ovarian follicles using ultrasound images [11].

Srivastava et al. [12] proposed a novel approach for detecting ovarian cysts in ultrasound images using a fine-tuned VGG-16 Deep Learning Network. By customizing the last four layers of the VGG-16 model with their dataset, they achieved an accuracy of 92.11%. This method shows promise for early cyst detection, which is crucial for timely intervention and preventing severe health complications such as torsion and infertility [12].

Satish et al. [13] explored PCOS classification and feature selection using machine learning techniques. Their study, utilizing Python-Scikit Learn and Rapid Miner, identified Random Forest as the most effective classification model, achieving 93.12% accuracy (Rapid Miner) with the complete dataset. KNN and SVM also demonstrated similar accuracies (90.83%, Rapid Miner) with 10 selected features. The study highlights the importance of feature selection in enhancing PCOS prediction models and notes that while Rapid Miner generally outperforms Python, the choice of tool depends on dataset characteristics and analytical needs [13].

Ramamoorthy and Sivasubramaniam [17] introduced a method for early detection and monitoring of PCOS using ultrasound abdomen scan images and image registration techniques. Their system includes Image Preprocessing, which removes speckle noise using the db2 wavelet filter, and Image Registration, which uses correlation coefficient similarity metrics and affine transformation to track cyst growth. The system achieved a 93% accuracy in detecting early-stage PCOS, aiding in timely diagnosis and treatment decisions. Future work aims to incorporate deep learning algorithms like CNNs to classify different PCOS stages based on factors such as stress and obesity [17].

 ISSN 2723-6471

In summary, the reviewed studies collectively highlight a range of methodologies for PCOS detection and diagnosis, from traditional image processing techniques to advanced deep learning algorithms. While some studies focus on automated follicle identification using ultrasound imaging, others explore machine learning and deep learning models for PCOS classification. Innovative methods like image registration techniques also show promise for early PCOS detection and monitoring. These advancements underscore the importance of ongoing research and collaboration in medical imaging and data analysis to improve PCOS diagnosis and treatment outcomes, ultimately enhancing women's health and fertility [1], [11], [12], [13], [17].

3. Classification Techniques

The physical symptoms like hair growth, acene and irregular periods, but these types of symptoms are not adequate to diagnosis PCOS [21]. Furthermore, the hormone test like Luteinizing hormone, androgen, Follicle stimulating hormone, DHEAS, blood sugar and insulin should be Inspected. The hormone and physical symptoms considered as a propose systems, so statistically analyzed of features with machine learning techniques. The figure 1 show that proposed method of mathematical formulation and the parameters like height, weight, age, sonography and fasting blood sugar.

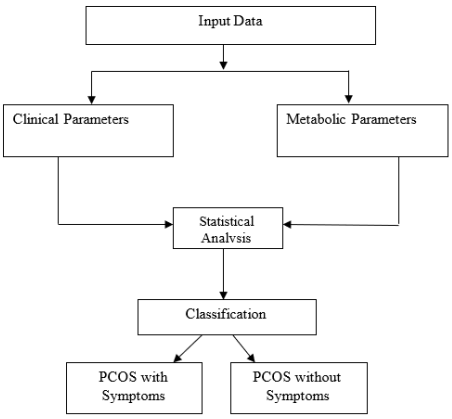

Figure 1. System Architecture

3.1. Dataset

The PCOS dataset generated has totally 13 attributes and 2 classes, so the instance is using 40 numbers have to be created. A total number of attributes based on the PCOS symptoms like patient's age, weight, height, skip or irregular periods, blood test, androgen, DHEAS, Follicle stimulating hormone, and blood sugar. The symptoms sonography, LH, irregular periods and weight are more important causes of PCOS, so the symptoms attributes are going to predict the PCOS or not.

3.2. Random Forest

This technique was developed and initiates [12] both the procedure of bagging idea and random feature selection. This method is used to compute the distribution of estimator is related to data sampling and swapping from original dataset. In this method, the sample is associated with n is occupied from training data and this model to produce the new data and replacing the actual data [22]. Furthermore, the random features allow random features selection subset in each and every node. The random features to improve the better accuracy rate for data prediction. The formula as follows:

$$\rho\sigma^2 + \frac{1-\rho}{K}\sigma^2 \quad (1)$$

Note: σ2 - tree variance, ρ - Correlation between trees, K - Total trees.

3.3. Logistic Regression

Among this model connection with binary outcomes and independent variables based on the probability as dependent variables of forecast value. In this proposed, every feature was verified and assigned a value, so the data wad classified the PCOS test results of normal or PCOS. Suppose the probability is higher than the PCOS threshold else normal women [14]. The formula as follow as:

 ISSN 2723-6471

$$\pi(X) = \frac{1}{1} + e^{-y} \quad (2)$$

where y denotes coefficients variable, e is representing Euler's.

3.4. Bayesian Classifier

The probabilistic classifier utilizes Bayes' theorem to make predictions. A Bayesian classifier estimates the probability of a feature belonging to a particular class, even if the class is unknown or if only some features are known. The probabilities of features, learned from training data, are used in classification methods. The Bayesian classifier is commonly referred to as the Naïve Bayes classifier. One of the key assumptions of the Naïve Bayes classifier is that the value of a feature is considered to be independent of the values of other features. This implies that there is zero correlation among features, meaning that the presence or absence of one feature does not affect the presence or absence of another feature. While this assumption simplifies the computation, it may not accurately reflect the relationships between features in real-world data, where features often exhibit some level of interdependence [23].

Another assumption is that all features are treated as equally important and are given equal weight in the classification process. This means that the classifier does not prioritize any particular feature over others, and each feature contributes equally to the final classification decision. This approach can be beneficial for simplifying the model and reducing computational complexity, but it may overlook the varying degrees of relevance that different features might have in distinguishing between classes. Naïve Bayes classifiers can be categorized into different types based on the nature of the features and the assumptions made about their distribution. The Multinomial Naïve Bayes classifier is typically used for discrete data and is well-suited for text classification tasks. The Gaussian Naïve Bayes classifier assumes that features follow a Gaussian (normal) distribution and is often used for continuous data. The Bernoulli Naïve Bayes classifier, on the other hand, is designed for binary or Boolean features, making it suitable for tasks where features are either present or absent. Each type of Naïve Bayes classifier has its own strengths and is chosen based on the specific characteristics of the data being analyzed [24].

3.5. Support Vector Machine

The main objectives of above technique are used to divide dataset is better decision. The margin consists of distance between the nearest points. The purpose of this hyper-lane to select a maximum marginal between the support vectors in the following datasets. To search a maximum marginal hyper-lane is given as:

$$s(x) = \text{sign} \sum_{k} a - \text{kykK}(\text{xk}, x) + b) \quad (3)$$

(a) To generate hyper-lane is best way to divide classes. In below figure showing three hyper-lanes blue, black and orange. A higher classification error consists of orange and blue. The black is dividing the two classes. Figure 2 illustrates the concept of hyperplanes within a multidimensional space, highlighting their role in classification tasks such as those performed by SVMs. A hyperplane is a subspace that separates different classes in a dataset; in two dimensions, it appears as a line, while in three dimensions, it takes the form of a plane. In higher dimensions, it generalizes to a more abstract concept. The structure shown demonstrates how hyperplanes divide the feature space into distinct regions, with the optimal hyperplane being selected to maximize the margin—the distance between the hyperplane and the nearest data points from each class [25]. This maximization enhances the model's ability to generalize and improve classification performance by clearly delineating the boundaries between different classes.

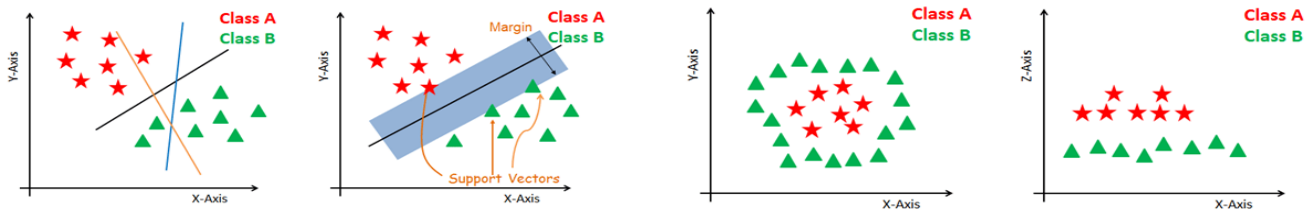

Figure 2. Structure of Hyper Planes

A kernel method is using an input space is transformed to high dimensional space. There are two data point is plotted on x and z-axis. The squared of z-axis is used with sum of both axis x and y: z=x^2=y^2. At the present it can simply separates all the points using linear separation.

 ISSN 2723-6471

3.6. Artificial Neural Network

Figure 3 illustrates the fundamental architecture of an Artificial Neural Network (ANN), showing its layered structure and the data flow within the network. The ANN is organized into three main layers: the input layer, hidden layers, and output layer. The input layer receives the raw data, which is then processed through one or more hidden layers. In these hidden layers, neurons apply weights and activation functions to learn complex patterns from the data. Finally, the output layer produces predictions or classifications based on the processed information. Connections between neurons are weighted, and these weights are adjusted during training to enhance the network's performance.

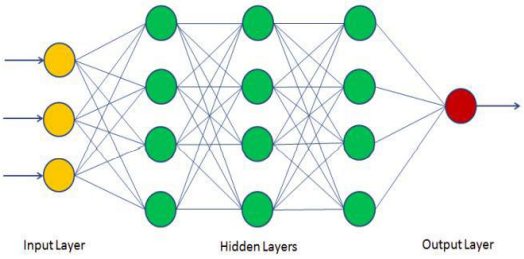

Figure 3. Basic Structure of ANN

The application of the ANN model combined with an improved fruit fly optimization approach (IFFOA) was proposed [17]. This model performed resizing of ultrasonic input images and noise elimination to enhance image quality. Adaptive k-means clustering was employed for follicle segmentation, while statistical Gray-Level Co-occurrence Matrix (GLCM) techniques were used for feature extraction. The ANN model was then trained with these refined features, leading to improvements in precision, recall, and accuracy in the classification results.

3.7. Convolutional Neural Network

In this part, a deep learning model-based PCOS diagnosis is proposed. Convolutional neural networks' primary contribution, in comparison toother network topologies, is accuracy. Diverse training techniques, however, have been devised to enhance performance servicing several CNN architectures. These designs perform better than conventional CNNs. In this work, we identify PCOS characteristics from medical photos using the deep CNN architecture VGG-19 (Visual Geometry Group). By substituting several tiny kernel size filters for big kernel size filters, the VGG Net model performs better than Alex Net. To enhance the detection performance of deep learning models, support vector machines should be used rather than fully connected network designs. Figure 4 depicts the suggested network model's design.

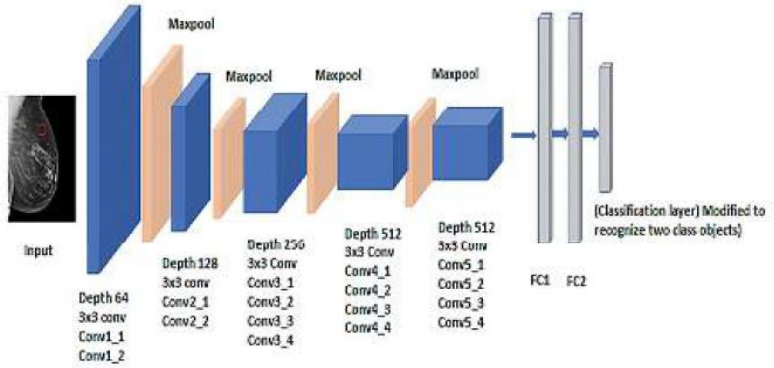

Figure 4. VGG-19 network architecture

There are 19 layers in the VGG-19 network design, 16 of which are convolutional layers and 3 of which are fully linked layers. Deep neural networks are more precise because they can process information with greater accuracy as they gain more layers. Convolutional layers conduct convolutional operations, are connected to max-pooling and dropout layers, and are fully depth-trainable. Max pooling is used to minimize the output size of the convolutional layer, which is just a 3x3 network layer. A single lesion is used to train and test the proposed network to eliminate false positives. Each pixel of the input picture is subjected to a convolution operation by a convolutional layer, which then transmits the results to the following layer. Following convolution, an image with n features is produced. These features are derived using the kernel function of the convolution layer. The mathematical expression for a convolutional layer's output as

 ISSN 2723-6471

$$m_i^{(x)} = B_i^{(x)} + \sum_{j=1}^{b_i^{(x-1)}} k_{i,j}^{(x-1)} \text{ x } m_j^{(x)} \quad (4)$$

The feature map is the output function generated by passing, where $k_{i,j}^{(x-1)}$denotes the convolution kernel or filter size, $B_i^{(x)}$ denotes matrix deflection, and $m_i^{(x)}$is the convolution kernel size. After the convolution procedure, theactivation function is used to create a nonlinear transfer function, which isrepresented by

$$n_i^{(x)} = n\,(m_i^{(n)}) \quad (5)$$

$n_i^{(x)}$here stands for the activation function. Many activation functions areaccessible, including the sigmoid function, the hyperbolic tangent function, and theReLU (Rectified Linear Unit) function, which is popular because to its high computing efficiency. The mathematical representation of the ReLU function as

$$n_i^{(x)} = \max(0, n_i^{(x)}) \quad (6)$$

In order to minimize interaction with nonlinear effects, the activation function only handles positive values and substitutes negative values with zeros. Max pooling or sampling layers are employed in addition to convolutional layers to minimize the size of the convolutional output. The suggested work employs max pooling, which considers the maximum value of each block as the output picture pixel. Max pooling is one of three main types of sampling processes: average pooling, sum pooling, and max pooling. Three networks make to theVGG-19's overall architecture. The formula for the SoftMax activation function in this hierarchy, which is used to categorize features using the feed-forward neural network,

$$n_i^{(x)} = f(x_i^{(x)}) \quad (7)$$

Where, f is the nonlinear transfer function and is the weighting function. Instead of utilizing a feed-forward neural network for the job we propose, we categorize tumor status using a straightforward and effective support vector machine. Support vector machines outperform other machine learning classifiers in terms of classification performance. SVM analyses the smallest features for the best accuracy since a deep network chooses the fundamental characteristics. The ideal hyperplane for dividing the feature space is found through supervised learning methods. The training dataset should be split up into classes using a high dimensional hyperplane. A kernel-aware vector machine is used to move nonlinearly separable data into a new vector space. The decision linear classification function is stated as follows given the training data set

$$D(x_1, y_1), (x_2, y_2), (x_2, y_2), \ldots, (x_n, y_n).$$
$$y_i = ((w\Delta x_i + b) \quad (8)$$

The suggested architecture's detailed hierarchical structure is outlined in table 1 provides a detailed breakdown of the proposed convolutional neural network (CNN) architecture, outlining the specifics of each layer used in the model. The network begins with two convolutional layers, Conv1_1 and Conv1_2, both with a size of 224x224 pixels and 64 feature maps, utilizing a 3x3 kernel and ReLU activation function. Following these layers is a max pooling layer, which reduces the spatial dimensions to 112x112 pixels and doubles the feature map count to 128.

Table 1. Proposed architecture layer details

Layer	Size	Kernel size	Feature map	Stride	Activation
Conv1_1	224x224x64	3x3	64	1	ReLU
Conv1_2	224x224x64	3x3	64	1	ReLU
Max pooling	112x112x64	3x3	128	2	ReLU
Conv2_1	112x112x128	3x3	128	1	ReLU
Conv2_2	112x112x128	3x3	128	1	ReLU
Max pooling	56x56x128	3x3	128	2	ReLU
Conv3_1	56x56x256	3x3	256	1	ReLU

 ISSN 2723-6471

Conv3_2	56x56x256	3x3	256	1	ReLU
Conv3_3	56x56x256	3x3	256	1	ReLU
Conv3_4	56x56x256	3x3	256	1	ReLU
Max pooling	28x28x256	3x3	256	2	ReLU
Conv4_1	28x28x512	3x3	512	1	ReLU
Conv4_2	28x28x512	3x3	512	1	ReLU
Conv4_3	28x28x512	3x3	512	1	ReLU
Conv4_4	28x28x512	3x3	512	1	ReLU
Max pooling	7x7x512	3x3	512	2	ReLU
Conv3_1	7x7x512	3x3	512	1	ReLU
Conv3_2	7x7x512	3x3	512	1	ReLU
Conv3_3	7x7x512	3x3	512	1	ReLU
Conv3_4	7x7x512	3x3	512	1	ReLU
FCN 1	25088	-	-	-	ReLU
FCN 2	4096	-	-	-	ReLU
FCN	1000	-	-	-	Softmax

The architecture continues with two sets of convolutional layers (Conv2_1 and Conv2_2, Conv3_1 through Conv3_4, and Conv4_1 through Conv4_4), each progressively increasing the depth and complexity of the network. The Conv2 and Conv3 blocks introduce 128 and 256 feature maps, respectively, with the same 3x3 kernel size and ReLU activation. Max pooling layers follow, further downsampling the feature maps and reducing spatial dimensions to 56x56, 28x28, and finally 7x7 pixels.

In the final stages, fully connected layers (FCN 1 and FCN 2) process the flattened feature maps, with FCN 1 having 25088 units and FCN 2 containing 4096 units, both using ReLU activation. The output layer (FCN) consists of 1000 units with a Softmax activation function, providing the final classification scores. This architecture is designed to capture and learn complex features from input images, progressively refining the spatial and feature representation through convolutional, pooling, and fully connected layers.

4. Result and Discussion

The objective of this research work involves various machine learning techniques to identify the suitable algorithm for classified the dataset. The machine learning algorithms like Random Forest, Logistic Regression, Bayesian Classifier, Support Vector Classifier, Artificial Neural Network and CNN are used for classified dataset and the performance analyzed the statistical features. All features are performed based on the time duration. The statistical features like Correlation Coefficient, mean absolute error (MAE), root mean squared error (RMSE) and relative absolute error (RAE). The parameter is calculated and compared using MATLAB tool. Table 2 provides a comprehensive comparison of various classification techniques based on their performance metrics, including classification time, correlation coefficient, MAE, RMSE, and RAE. The Random Forest classifier demonstrated a reasonable classification time of 0.57 seconds and achieved a high correlation coefficient of 0.9938, indicating strong predictive accuracy. It recorded an MAE of 0.015 and an RMSE of 0.0525, with an RAE of 3.22, reflecting moderate error levels.

Table 2. Classification Test Results with Statistical Features

Techniques	Time (sec)	Correlation Coefficient	MAE	RMSE	RAE
Random Forest	0.57	0.9938	0.015	0.0525	3.22
Logistic Regression	0	1	0.0001	0.0004	2.13
Bayesian Classifier	0	0.9755	0.0129	0.1081	2.34

 ISSN 2723-6471

Support Vector Machine	0	0.9328	0.0459	0.17	8.90
Artificial Neural Network	0.12	0.979	0.002	0.1422	5.74
VGG 19	0.36	1	0.003	0.0001	0.01

In contrast, Logistic Regression exhibited an impressive performance with a classification time of 0 seconds, a perfect correlation coefficient of 1, and minimal MAE (0.0001) and RMSE (0.0004), resulting in the lowest RAE of 2.13. The Bayesian Classifier, with a zero-classification time, achieved a correlation coefficient of 0.9755, an MAE of 0.0129, and an RMSE of 0.1081, yielding an RAE of 2.34. The Support Vector Machine (SVM) showed a classification time of 0 seconds but had a correlation coefficient of 0.9328, with higher MAE (0.0459) and RMSE (0.17), and a relatively high RAE of 8.90. The Artificial Neural Network (ANN) achieved a classification time of 0.12 seconds, a correlation coefficient of 0.979, an MAE of 0.002, and an RMSE of 0.1422, with an RAE of 5.74. Notably, the VGG 19 model demonstrated a classification time of 0.36 seconds and a perfect correlation coefficient of 1, with an MAE of 0.003, an exceptionally low RMSE of 0.0001, and the lowest RAE of 0.01, indicating superior accuracy and error minimization. Overall, Logistic Regression and VGG 19 exhibited the best performance in terms of accuracy and error metrics, while SVM presented relatively higher error rates. Figure 5 illustrates the line graph depicting the classification test results for various techniques, showcasing their performance metrics, including correlation coefficient, MAE, RMSE, and RAE. This visual representation highlights the comparative effectiveness of each technique in terms of accuracy and error, providing a clear overview of their relative performance.

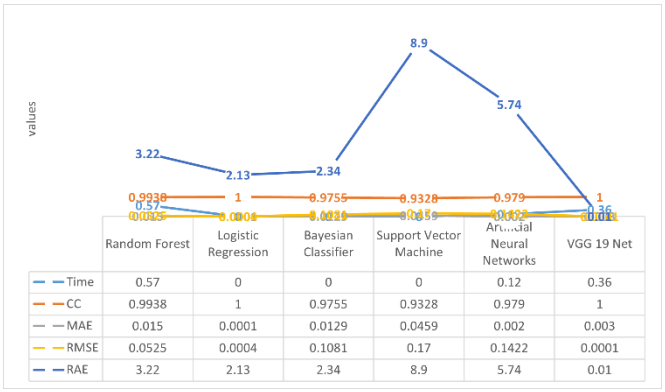

Figure 5. Line Graph for Classification Test Results with Statistical Features

From test analysis the graphical representation of various classification algorithms using statistical parameters. The comparative analysis and reviewing of various classification techniques to found the best accuracy rate. TheVGG19 Net techniques are given better accuracy rate to compare with other classification techniques. Table 3 presents the classification reports for various techniques, evaluating their performance across several metrics: precision, recall, F-score, and overall accuracy.

Table 3. Classification Reports of Various Techniques

Techniques	Precision (Class 1)	Recall (Class 1)	F Score (Class 1)	Accuracy
Random Forest	0.91	0.92	0.92	0.94
Logistic Regression	0.89	0.95	0.91	0.93
Bayesian Classifier	0.88	0.93	0.91	0.81
Support Vector Machine	0.83	0.93	0.90	0.92
Artificial Neural Network	0.81	0.93	0.83	0.90
VGG 19	0.89	0.97	0.92	0.96

The Random Forest model achieved a precision of 0.91, a recall of 0.92, and an F-score of 0.92, with an overall accuracy of 0.94. Logistic Regression demonstrated slightly lower precision at 0.89 but excelled in recall with 0.95 and achieved an F-score of 0.91, resulting in a high accuracy of 0.93. The Bayesian Classifier showed a precision of 0.88, recall of 0.93, and an F-score of 0.91, but had a lower accuracy of 0.81 compared to other models. The SVM recorded a precision

 ISSN 2723-6471

of 0.83 and a recall of 0.93, with an F-score of 0.90 and an accuracy of 0.92. The Artificial Neural Network (ANN) achieved a precision of 0.81, recall of 0.93, and an F-score of 0.83, with an accuracy of 0.90. Notably, the VGG 19 model performed the best with a precision of 0.89, recall of 0.97, and an F-score of 0.92, attaining the highest accuracy of 0.96. This table provides a comprehensive view of how each technique performs in classifying instances, highlighting their strengths and limitations in terms of precision, recall, F-score, and accuracy. Figure 6 illustrates a comparative analysis of various machine learning algorithms used for diagnosing Polycystic Ovary Syndrome (PCOS), with a focus on the performance ratios of Class 1. This figure visualizes how different algorithms—such as Random Forest, Logistic Regression, Bayesian Classifier, Support Vector Machine, Artificial Neural Network, and VGG 19—perform relative to each other in terms of their ability to classify instances of PCOS. By examining the Class 1 ratio, the figure provides insights into the effectiveness and efficiency of each algorithm in accurately diagnosing PCOS, highlighting their comparative strengths and weaknesses in this diagnostic application.

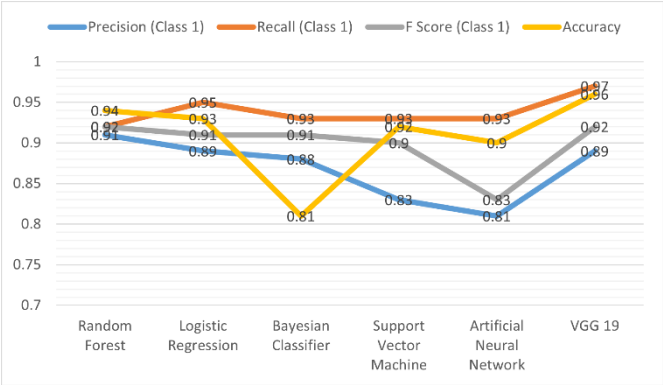

Figure 6. Comparative analysis of machine learning algorithms in diagnosis of PCOS Using Class 1 Ratio

Table 3 show that the report on various classification techniques using Recall, F-score and Precision of class1. The VGG 19 Net is better accuracy rate compared with other classification techniques. Table 4 presents a comprehensive classification report for various machine learning techniques, focusing on their performance in identifying Class 2 instances.

Table 4. Classification Reports of Various Techniques

Techniques	Precision (Class 2)	Recall (Class 2)	F Score (Class 2)	Accuracy
Random Forest	0.84	0.84	0.84	0.94
Logistic Regression	0.87	0.90	0.92	0.91
Bayesian Classifier	0.88	0.81	0.86	0.81
Support Vector Machine	0.90	0.91	0.90	0.92
Artificial Neural Network	0.80	0.92	0.84	0.90
VGG 19	0.94	0.80	0.86	0.96

Among the techniques evaluated, Random Forest achieved a Precision of 0.84, Recall of 0.84, and an F Score of 0.84, with an Accuracy of 0.94, indicating strong overall performance with a high accuracy. Logistic Regression demonstrated a Precision of 0.87 and a Recall of 0.90, yielding a high F Score of 0.92 and an Accuracy of 0.91, reflecting its effective classification of Class 2 while maintaining robust performance metrics. The Bayesian Classifier showed a Precision of 0.88 and a Recall of 0.81, resulting in an F Score of 0.86 and an Accuracy of 0.81, highlighting good precision but slightly lower recall and overall accuracy compared to some techniques. The Support Vector Machine exhibited a Precision of 0.90, a Recall of 0.91, and an F Score of 0.90, with an Accuracy of 0.92, indicating a well-rounded performance with high precision and recall. Artificial Neural Network recorded a Precision of 0.80 and a Recall of 0.92, leading to an F Score of 0.84 and an Accuracy of 0.90, showing high recall but slightly lower precision.

 ISSN 2723-6471

Lastly, VGG 19 achieved the highest Precision of 0.94 and an Accuracy of 0.96, with a Recall of 0.80 and an F Score of 0.86, demonstrating exceptional precision and overall accuracy in Class 2 classification. This table highlights the varied strengths of each technique, with VGG 19 and Logistic Regression standing out for precision and accuracy, while Support Vector Machine and Bayesian Classifier provide balanced performance across metrics. Figure 7 provides a comparative analysis of different machine learning algorithms based on their performance in diagnosing PCOS, specifically focusing on the metrics related to Class 2 instances. The figure visually represents the effectiveness of each algorithm, including Random Forest, Logistic Regression, Bayesian Classifier, Support Vector Machine, Artificial Neural Network, and VGG 19, in distinguishing Class 2 cases. By illustrating key performance indicators such as Precision, Recall, F Score, and Accuracy, this figure highlights how each algorithm fares in the context of Class 2 classification, allowing for an easy comparison of their strengths and weaknesses.

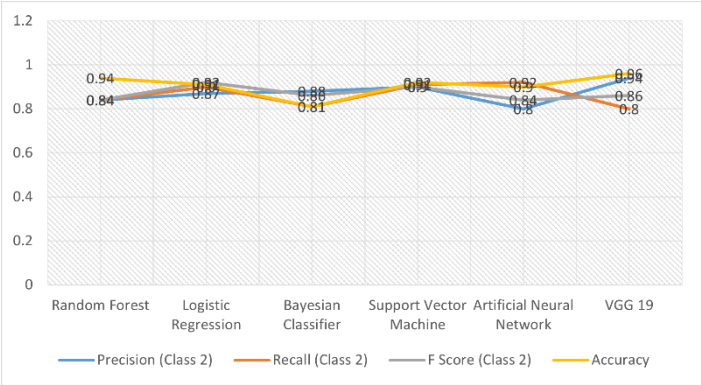

Figure 7. Comparative analysis of machine learning algorithms in diagnosis of PCOS Using Class 2 Ratio

5. Conclusion

This paper delves into the comparative effectiveness of various classification techniques for the early detection of PCOS, focusing on Random Forest, Logistic Regression, Bayesian Classifier, SVM, Artificial Neural Network (ANN), and VGG 19 Net. Utilizing real-time data provided by medical centers, the study aimed to evaluate and compare these algorithms based on their ability to accurately classify normal and abnormal conditions related to PCOS. Our analysis reveals that VGG 19 Net outperforms other techniques with an impressive accuracy of 96%, supported by a high precision of 0.94 and a recall of 0.80 for Class 2, indicating its robustness in detecting PCOS. The Random Forest model follows with an accuracy of 94%, demonstrating strong performance with a precision of 0.91 and a recall of 0.84 for Class 1. Logistic Regression and SVM also show effective performance with accuracies of 91% and 92%, respectively, but slightly lower precision and recall rates compared to VGG 19 Net. Specifically, Logistic Regression achieved a precision of 0.89 and recall of 0.95 for Class 1, while SVM had a precision of 0.83 and recall of 0.93 for the same class. The Bayesian Classifier and ANN, while useful, exhibited lower accuracy rates of 81% and 90%, respectively. The Bayesian Classifier had a precision of 0.88 and recall of 0.81 for Class 2, whereas the ANN achieved a precision of 0.80 and recall of 0.92. These findings underscore the superiority of the VGG 19 Net model in terms of accuracy and reliability. Its ability to achieve the highest classification performance highlights its potential as a valuable tool for early PCOS detection. This model's enhanced precision and recall rates enable more accurate diagnoses and facilitate earlier intervention, which is crucial for improving treatment outcomes and managing PCOS effectively. The comparative analysis demonstrates that while other algorithms perform well, VGG 19 Net's exceptional results make it particularly advantageous for medical applications where accuracy and early detection are paramount.

6. Declaration

6.1. Author Contributions

Conceptualization: M.P., N.N., S.S.M., and W.G.; Methodology: N.N., and M.P.; Software: M.P.; Validation: M.P., N.N., S.S.M., and W.G.; Formal Analysis: M.P., N.N., S.S.M., and W.G.; Investigation: M.P., S.S.M., and W.G.; Resources: S.S.M., and W.G.; Data Curation: S.S.M.; Writing Original Draft Preparation: M.P., N.N., S.S.M., and

W.G.; Writing Review and Editing: M.P., N.N., S.S.M., and W.G.; Visualization: M.P.; All authors have read and agreed to the published version of the manuscript

6.2. Data Availability Statement

The data presented in this study are available on request from the corresponding author.

6.3. Funding

The authors received no financial support for the research, authorship, and/or publication of this article.

6.4. Institutional Review Board Statement

Not applicable.

6.5. Informed Consent Statement

Not applicable.

6.6. Declaration of Competing Interest

The authors declare that they have no known competing financial interests or personal relationships that could have appeared to influence the work reported in this paper.

References

[1] A. A. Nazarudin, N. Zulkarnain, A. Hussain, S. S. Mokri, and I. N. Nordin, "Review on automated follicle identification for polycystic ovarian syndrome," *Bull. Electr. Eng. Informatics*, vol. 9, no. 2, pp. 588–593, 2020.

[2] C. V. Palm, D. Glintborg, H. B. Kyhl, H. D. McIntyre, R. C. Jensen, T. K. Jensen, D. M. Jensen, and M. Andersen, "Polycystic ovary syndrome and hyperglycaemia in pregnancy. A narrative review and results from a prospective Danish cohort study," *Diabetes Res. Clin. Pract.*, vol. 145, no. 1, pp. 167–177, 2018.

[3] H. F. Escobar-Morreale, "Polycystic ovary syndrome: Definition, aetiology, diagnosis and treatment," *Nat. Rev. Endocrinol.*, vol. 14, no. 5, pp. 270–284, 2018.

[4] M. Otaghi, M. Azami, A. Khorshidi, M. Borji, and Z. Tardeh, "The association between metabolic syndrome and polycystic ovary syndrome: A systematic review and meta-analysis," *Diabetes Metab. Syndr. Clin. Res. Rev.*, vol. 13, no. 2, pp. 1481–1489, 2019.

[5] E. Tassone, H. Teede, A. Dokras, R. Garad, and M. Gibson-Helm, "The needs of women and healthcare providers regarding polycystic ovary syndrome information, resources, and education: A systematic search and narrative review," *Semin. Reprod. Med.*, vol. 36, no. 1, pp. 35–41, 2018.

[6] P. Soni and S. Vashisht, "Image segmentation for detecting polycystic ovarian disease using deep neural networks," *Int. J. Comput. Sci. Eng.*, vol. 7, no. 3, pp. 534–537, 2019.

[7] S. Patel, "Polycystic ovary syndrome (PCOS), an inflammatory, systemic, lifestyle endocrinopathy," *J. Steroid Biochem. Mol. Biol.*, vol. 182, no. 1, pp. 27–36, 2018.

[8] Q. Zhang, Z.-k. Bao, M.-x. Deng, Q. Xu, D.-d. Ding, M.-m. Pan, X. Xi, F.-f. Wang, Y. Zou, and F. Qu, "Fetal growth, fetal development, and placental features in women with polycystic ovary syndrome: Analysis based on fetal and placental magnetic resonance imaging," *J. Zhejiang Univ.-SCI B*, vol. 21, no. 12, pp. 977–989, 2020.

[9] M. Sumathi, P. Chitra, R. Sakthi Prabha, and K. Srilatha, "Study and detection of PCOS related diseases using CNN," *IOP Conf. Ser.: Mater. Sci. Eng.*, vol. 1070, no. 1, pp. 012-062, 2021.

[10] B. Y. Jarrett, H. Vanden Brink, A. L. Oldfield, and M. E. Lujan, "Ultrasound characterization of disordered antral follicle development in women with polycystic ovary syndrome," *J. Clin. Endocrinol. Metab.*, vol. 105, no. 11, pp. e3847–e3861, 2020.

[11] P. G. YILMAZ and G. ÖZMEN, "Follicle detection for polycystic ovary syndrome by using image processing methods," *Int. J. Appl. Math. Electron. Comput.*, vol. 8, no. 4, pp. 203–208, 2020.

[12] S. Srivastava, P. Kumar, V. Chaudhry, and A. Singh, "Detection of ovarian cyst in ultrasound images using fine-tuned VGG-16 Deep Learning Network," *SN Comput. Sci.*, vol. 1, no. 2, pp. 1–8, 2020.

[13] C. N. Satish, X. Chew, and K. W. Khaw, "Polycystic Ovarian Syndrome (PCOS) classification and feature selection by machine learning techniques," *Appl. Math. Comput. Intell.*, vol. 9, no. 1, pp. 65–74, 2020.

 ISSN 2723-6471

[14] U. A. Ndefo, A. Eaton, and M. R. Green, "Polycystic Ovary Syndrome, A Review of Treatment Options With a Focus on Pharmacological Approaches," *Jun.*, vol. 38, no. 6, pp. 336–338, 348, 355, 2013.

[15] N. Thomas and A. Kavitha, "A Literature Inspection on Polycystic Ovarian Morphology in Women using Data Mining Methodologies," *Int. J. Adv. Res. Comput. Sci.*, vol. 9, no. 1, pp. 158–162, Jan.-Feb. 2018.

[16] P. Rajkumari, J. Sahoo, P. Sujata, G. Sahoo, and J. Hansa, "Awareness about PCOS and the likelihood of its symptoms in adolescent girls in a semi-urban set-up: A cross sectional study," J. Med. Sci. Clin. Res., vol. 4, no. 1, pp. 14264-14269, 2016.

[17] S. Ramamoorthy and R. Sivasubramaniam, "Monitoring the growth of Polycystic Ovary Syndrome using Mono-modal Image Registration Technique: Application of Medical Big Data in Healthcare," in *Proc. ACM India Joint Int. Conf. Data Sci. Manag. Data*, vol. 2019, no. 1, pp. 180–187, 2019.

[18] C. E. Cesta, A. S. Öberg, A. Ibrahimson, I. Yusuf, H. Larsson, C. Almqvist, B. M. D'Onofrio, C. M. Bulik, L. Fernández de la Cruz, D. Mataix-Cols, M. Landén, and M. A. Rosenqvist, "Maternal polycystic ovary syndrome and risk of neuropsychiatric disorders in offspring: Prenatal androgen exposure or genetic confounding?" *Psychol. Med.*, vol. 50, no. 4, pp. 616–624, 2019.

[19] G. Bozdag, S. Mumusoglu, D. Zengin, E. Karabulut, and B. O. Yildiz, "The prevalence and phenotypic features of polycystic ovary syndrome: A systematic review and meta-analysis," *Hum. Reprod.*, vol. 31, no. 12, pp. 2841–2855, 2016.

[20] A. Kumar, R. S. Umurzoqovich, N. D. Duong, P. Kanani, A. Kuppusamy, M. Praneesh, and M. N. Hieu, "An intrusion identification and prevention for cloud computing: From the perspective of deep learning," *Optik*, vol. 270, no. 1, pp. 170044-170052, 2022.

[21] J.P.B. Saputra andS. Yadav, "Modeling the Impact of Holidays and Events on Retail Demand Forecasting in Online Marketing Campaigns using Intervention Analysis," *J. Digit. Mark. Digit. Curr.*, vol. 1, no. 2, pp. 144-164, 2024.

[22] N. Boonsatit, S. Rajendran, C. P. Lim, A. Jirawattanapanit, and P. Mohandas, "New adaptive finite-time cluster synchronization of neutral-type complex-valued coupled neural networks with mixed time delays," *Fractals*, vol. 6, no. 9, pp. 515-524, 2022.

[23] A. R. Yadulla, M. H. Maturi, K. Meduri, G. S. Nadella, "Sales Trends and Price Determinants in the Virtual Property Market: Insights from Blockchain-Based Platforms," *Int. J. Res. Metav.*, vol. 1, no. 2, pp. 113-126, 2024.

[24] Hery and A. E. Widjaja, "Predictive Modeling of Blockchain Stability Using Machine Learning to Enhance Network Resilience", *J. Curr. Res. Blockchain.*, vol. 1, no. 2, pp. 124–138, Sep. 2024.

[25] Y. Wei et al., "Comparative Analysis of Artificial Intelligence Methods for Streamflow Forecasting," *IEEE Access*, vol. 12, no. 1, pp. 10865–10885, 2024, doi: 10.1109/ACCESS.2024.3351754.